Effect of coupling agents on the degradation of Polypropylene/fly ash composites

Christopher Mark Liauw[a], Itziar Iraola-Arregui[a1], Johannes Herman Potgieter[b*]

[a] School of Engineering, Manchester Metropolitan University, Manchester, M1 5GD, UK.

[b] School of Research Enterprise and Innovation, Manchester Metropolitan University, Manchester, M1 5GD, UK.

[1] Consolidation of Metallic and Ceramic Powders, CEIT-IK4 Research Alliance, San Sebastián, 20.018, SPAIN.

* Corresponding author: h.potgeiter@mmu.ac.uk; tel: 0044 (0)161 247 1428

ABSTRACT

Composites containing 50 % wt fly ash (sourced from the UK and South Africa) in polypropylene homopolymer (manufacturer stabilised for general purpose use) have been prepared by using batch and continuous methods. The effect of the following coupling agents were investigated on the photo- and thermal decomposition of the composite materials.: Lubrizol Solplus C800 (an unsaturated carboxylic acid), γ-Methacryloxypropyl trimethoxy silane (γ-MPS), 1,3-phenylene dimaleimide (BMI) and maleic anhydride grafted polypropylene (m-PP) High melt, thermal and photo stability was favoured when the matrix was coupled to the filler surface by monomeric coupling agents that were expected to adsorb in a close packed layer on the fly ash surface. Further improvements were observed in cases where the coupling agent could also self-polymerise. m-PP did not lead to increased stability due to its low adsorption density on the fly ash surface. The relatively high water / acid soluble transition metal ion content of the UK sourced fly ash did not appear to affect stability under the test conditions employed in this study. The South African sourced fly ash had a higher level of quartz and mullite together with a high level of group 1 and 2 metals. The latter in particular may have led to debonding of the coupled interfacial region from the filler surface and possible adsorption of stabilisers on the pristine surface. This resulted in the South African fly ash generally possessing poorer resistance to oxidation than the UK fly ash.

INTRODUCTION

Most plastic materials are used because they have desirable mechanical properties at an economical cost. Plastics are mainly composed of polymers and some other substances (additives or modifiers) added in order to improve performance and/or reduce costs, such as fillers stabilizers, pigments, flame retardants, etc.[1] Polypropylene (PP) is one of the most versatile thermoplastics and is used in a large number of applications ranging from films, packaging, tubing and textiles, to automotive components. Factors contributing to such prolific consumption include its excellent price/property relationship, good fabrication possibilities and the ability to modify its mechanical properties. The performance of PP can be boosted substantially via use of reinforcing fillers, such as talc and short glass fibres. Other properties, e.g. reduction in mould shrinkage, can be improved via addition of low cost non-reinforcing fillers such as calcium carbonate.[2-4]

It is well established that fillers can affect the stability, crystallinity and other properties of the PP. This effect depends on many factors, such as the presence of surface treatments (coupling agents and dispersants) and impurities (such as transition elements). Formulation dependent factors include filler volume fraction (the level of filler will affect the melt shear stress and hence the level of mechanical chain scission), and the specific type of PP (i.e. the presence of co-monomers and the catalyst system used). Some of these effects can be overcome by treating the filler particles with additives (coupling agents) that modify the surface characteristics of the filler. Coupling agents are often used to increase the strength of particulate filled polymer composites.[5,6] They increase the strength of interaction between the filler surface and the matrix. At

high filler levels an increase in interfacial adhesion can give a better composite strength – toughness balance than dispersant type treatments that merely increase filler dispersion quality at the expense of interfacial adhesion.[7]

Some interesting effects have been found in the thermo-oxidation of filled PP . Jiangqing et al.[8] found that the impurities of the filler caused an increase in the degradation rate of the composite material. Suradi et al.[9] reported that the benefits of the coupling agent resolve the interfacial adhesion problems and thus improve the degradation. Chen et al.[10] observed that the filler used in their work had a positive effect on the degradation mechanism of PP, as it was much more difficult to degrade the filled material than the unfilled PP homopolymer. Chen et al.[11] also studied the effect that transition metals have on the degradation of $Mg(OH)_2$ -PP composites. Selden et al.[12] reported that doubling the filler amount in the composite could lead to an increase in the degradation rate by up to a factor of two.

Embrittlement of non-stabilised PP occurs within a few days[13] of UV and/or thermal degradation in air. Therefore PP is a polymer whose commercial success could not be anything like it is today without stabilisers. All general purpose grades of PP are stabilised by the polymer producer / supplier. The thermal and photo-oxidation of PP has been well reviewed elsewhere[14,15], though the effect of fillers on the oxidation of PP has received much less attention.

In our previous work[16] we investigated the melt and mechanical properties of coupling agent treated fly ash-PP composites. It was found that the incorporation of a suitable filler surface treatment could improve the performance of the material. In the present

work, the effect of the different coupling agents on degradation and lifetime of the PP-fly ash composites will be described, taking into account different processing methods employed.

EXPERIMENTAL

Materials

Fly ash was obtained from Lethabo Power Station in South Africa (SuperPozz, an ultrafine fly ash) and was coded SAFA. A sample of filler grade fly ash was also supplied by Rocktron Limited, Bristol, UK. It was the Min-Tron Grade and was coded UKFA. Particles are spherical shaped and the average particle diameter is 3.2 for SAFA samples and of 3.1 μm for UKFA. The smallest particles showed some aggregation.

Coupling agents.

For this study, four different coupling agents were used:

(i)   γ-Methacryloxypropyltrimethoxy silane (γ-MPS), (Silquest® A 174 (GE Bayern Silicones))

(ii)   Maleanised polypropylene (m-PP) (Orevac® CA100 (Atofina (UK) Ltd.))

(iii)   N,N'-(1,3-phenylene) dimaleimide (BMI), (Aldrich Co. Ltd).

(iv)   Solplus® C800 (Note: the 50 wt.-% active silica supported form (Solplus® C825 was used in this study). C800 is an oligomeric unsaturated carboxylic acid type coupling agent that includes a sterically accessible double bond that is easily activated. (It´s structure is propietary). (Lubrizol Advanced Materials, Inc. (UK)).

Peroxide.

An organic peroxide was used as an initiator for C800, γ-MPS and BMI. The type chosen was dicumyl peroxide (DCP) as it has a half life ($t_{1/2}$) of 1 hour at 138 °C and is therefore most appropriate for the processing conditions used in this study. The grade of DCP selected was Akzo-Nobel Perkadox BC-40B, and it is 40 wt.-% active. The carrier is calcium carbonate.

Polypropylene.

The PP homopolymer matrix selected was Borealis HD120MO, a general purpose injection moulding grade with a melt flow rate (MFR) of 8 dg/min (230°C, 2.16 kg) (ISO 1133). It is understood that this PP contains a general purpose stabiliser package.

Determination of fly ash composition

Transition metal impurities in fillers have been known to accelerate the degradation of polypropylene.[17-20]. Inductive coupled plasma (ICP) spectroscopy was used to investigate the presence of transition metals in the fly ash samples. The metals were extracted under two sets of conditions which included mild aqueous leaching and more aggressive leaching in concentrated nitric acid.

For the aqueous leaching, fly ash (1 g) was added to a 400 ml beaker containing distilled water (100 ml). As the fly ash is not soluble in water, only the extractable ions on the surface of the fly ash sample can be analysed by this method. After stirring the mixture overnight, supernatant was removed from the suspension and filtered through a syringe filter. Distilled water was used as the blank sample.

Acid leaching with 69 % nitric acid was carried out using the same procedure as for the aqueous leaching. It was envisaged that the nitric acid may penetrate more deeply into the predominantly silica surface of the fly ash particles, and hence remove sub-surface

ions. The nitric acid solution was used as the blank sample. All determinations were performed in duplicate.

The equipment used for the metal trace analysis was an ICP-AES Spectrophotometer (VISTA AX, Varian), fitted with a Charged Coupled Device (CCD) detector. The torch used for creating the plasma was an axially mounted one piece quartz glass type, and sample introduction was conducted via a glass nebulizer and spray chamber.

Composite preparation

Batch melt (BM) mixing and compression moulding (CM) of test plaques.

The composites will from henceforth be denoted as BM-CM types. PP composites were prepared using a Thermo Haake Rheomix 600 mixing bowl fitted to a Haake Polydrive dynamometer unit. The bowl was fitted with Banbury type rotors. PP and fly ash were mixed for 10 minutes at a set temperature of 180°C with a rotor speed of 80 rpm to form composites containing 50% wt fly ash. Due to the liquid state of γ-MPS, the filler was pre-treated by mixing in a Waring blender for 1 minute. After removal from the Rheomix chamber, the composite melts were squashed between two steel plates, using a lever press, into a ca. 4 mm thick pre-form blank. The composite formulations are shown in Table 1.

Place table 1 here

Compression moulding of 102 mm x 102 mm x 3 mm composite test sheets was carried out using a 50 tonne press with electrically heated platens set at 190°C and a second press with water cooled platens for cooling the sample melt in the mould. The pre-form

blank was preheated in a mould that was in contact with the top platen of the press for 2 minutes before fully closing the mould for a further 2 minute period. The press was opened and the mould was then transferred to the water cooled press and full pressure was applied for 2 minutes. Test strips (50 mm x 10 mm x 3 mm) for degradation tests, were then cut from the compression moulded sheets using a band saw.

Preparation of test pieces by twin screw extrusion (TSE) and injection moulding(IM).

The latter composites will from henceforth be denoted as TSE-IM types. Formulations (2 kg total mass) were melt blended using a Thermo Prism HC 24 twin screw extruder (TSE). Composite formulations consisted of 50 wt.% polypropylene, similar amounts of UKFA and SAFA fly ashes in each case, and the further additions of 0.6 wt.% C800 and 0.05 wt. % DCP. The screw profile can be described as fairly harsh and features some reverse flow elements. However, subsequent SEM imaging of composite fracture surfaces revealed that the spherical fly ash particles remained intact. The polymer granules were fed to the feed zone of the screws using a single screw volumetric feeder and the filler (plus other powdered ingredients) were fed into the feed zone using a twin screw gravimetric feeder. The barrel was terminated with a three-hole strand die which fed into a cooling trough. The extrudate was hauled off and pelletised. Most of the water picked up by the extruded strands was removed with an air knife prior to entering the pelletiser.

Fly Ash, C800 coupling agent (as the 50 % wt active silica supported C825 form) and the DCP were tumble blended in a screw top tub prior to extrusion. The temperature profile of the extruder was as follows:

Feed End	Die End

Zone	1	2	3	4	5	6	7
Temperature(°C)	195	195	190	190	190	190	180

The screw speed was set at 300 rpm and the total output rate set nominally at 4.8 kg/h. The melt pressure at the die ranged from 5 bar of the pure polymer to 18 bar observed when compounding untreated filler with PP. The pellets were dried in an oven at 80ºC for 4h in order to remove any residual water that may have escaped removal by the air knife.

Composite pellets were injection moulded into tensile and impact test pieces (ISO R570) using a Battenfield BA 230CD Plus reciprocating screw injection moulding machine. The set temperature of all three zones was 200ºC. Injection pressure for the unfilled matrix was 35 Bar and for composites it was 50 Bar for unmodified and 45 Bar for C800/DCP modified materials. Hold pressure was 20 Bar for the unfilled matrix and 35 and 25 Bar for the unmodified and C800/DCP modified composites, respectively.

Composite Characterisation

Melt flow rate (MFR) was determined according to ISO 1133, at a temperature of 230°C and using a load of 2.16 kg. The compression moulded samples were hand cut by pliers into small pieces of around 4 mm x 4 mm x 3 mm. Unwanted portions of the injection moulded composites samples were converted into granules for MFR determination using a Rapid granulator. VMFR was used in order to make fair comparisons between the rate of flow of the filled and unfilled samples though the MFR die.

Volume melt flow-rate (VMFR, cm^3/10 min). The VMFR values were obtained by using the density values of the samples, as shown in Equation 1.

$$VMFR = \frac{m_{sample}/d_{sample}}{10\ min}$$
<div align="right">(1)</div>

Oxidation Induction Time (OIT).

A Perkin-Elmer DSC-7 power compensation type differential scanning calorimeter was used to measure the OIT of the PP / fly ash composites. Specimens were heated from 20ºC to 160ºC under a nitrogen atmosphere at 200ºC/min. The specimens were held at this temperature for five minutes to reach equilibrium. After this period of time, the gas flow was switched from nitrogen to oxygen. Oxidation was manifested as a negative (exothermic) deflection of the base line and the OIT is the time interval between switch over to oxygen and the onset time of the oxidation exotherm.

Thermal oxidative degradation.

Samples were exposed in a ventilated oven at 150°C. At appropriate time intervals (1, 2, 4, 6 and 8 h), the samples were taken out from the oven and the changes due to thermal oxidative degradation were monitored by FT-IR.

Photo-oxidative degradation.

Samples were exposed to a 500W high pressure Hg/W lamp (Philips ML 500W 235-245V) for 850h. Samples were removed from the unit every 50 h and changes were monitored by FT-IR.

Monitoring of oxidation using FT-IR.

Both the thermal and UV oxidised samples were checked for oxidation at the indicated time intervals using attenuated total reflectance (ATR) FT-IR. Oxidation of PP is

manifested as development of a group of carbonyl absorption bands in the range 1500 cm^{-1} to 1800 cm^{-1} [21] and development of OH stretching bands (3600-3200 cm^{-1}) due to formation of hydroperoxides and other OH functional species.

FT-IR quantification of the hydroperoxide concentration in the PP is potentially hampered by possible exposure of fly ash particles (which themselves show an OH stretching peak) at the degraded composite surface. Formation of carbonyl groups, however, was reliably monitored using FT-IR, as this area of spectrum was relatively free from artefacts and carbonyl growth was more prolific than hydroperoxide.

Several peaks, such as those at 840, 974, 1166 1455 and 2720 cm^{-1}, were found in the literature to be suitable for use as an internal standard for monitoring oxidation of PP[22,23]. The broad Si-O stretching band centred at around 1050 cm^{-1}, with the base of the peak extending down to 600 cm^{-1}, causes the peaks at 840, 974 and 1166 cm^{-1} to be unsuitable for use as internal standards for this study. The C-H deformation peak at 1455 cm^{-1} was therefore the most suitable internal standard, as it was not obscured by fly ash bands and is not significantly affected by the crystalline content or form of PP. A FTIR spectrum with the peaks used for the calculations are shown in Figure 1.

Place Figure 1 here.

A Thermo Nicolet 380 FT-IR fitted with a Smart Diamond single bounce diamond ATR cell was used for this analysis. Samples were clamped onto the diamond internal reflection element using the supplied self-regulating clamping system. Spectra were made up of 64 scans with resolution set to 4 cm^{-1}. The level of oxidation (carbonyl

growth) on the sample surfaces was quantified using the well known carbonyl index parameter (CI). Details of the carbonyl index and the reference peak calculations are expressed in Table 2.

Place table 2 here

All absorbance values were ratioed to the absorbance of the above internal standard to give a carbonyl index value (Equation 2).

$$CI = \frac{A_{C=O}}{A_{C-H}} \tag{2}$$

From the CI vs. time plots, $(t_{C=O})_{onset}$ was determined. An example showing the method used is given in **Figure 2**$(t_{C=O})_{onset}$ was calculated from the intersection of the line which best fits the slopes of the graph.

Place Figure 2 here.

Results and discussion

Oxidation Induction Time

OIT data for the BM-CM produced composites are presented in Figure 3.

Place Figure 3 here

The OIT data for the unmodified UKFA and SAFA based composites reveals contrasting pro-degradant (for the SAFA) and mild stabilising (for the UKFA) effects. Bearing in mind the acid leachable and ICP detectable transition metal content of

UKFA (see Table 3), this result is slightly unexpected. However, water/acid solubility of the transition metal content does not mean that it can be extracted by the polymer melt and it is highly likely that the transition metal content of UKFA was not accessible to the polymer during the OIT determination. The reduced OIT of SAFA may be related to greater tendency relative to UKFA to adsorb the antioxidants. This may be associated with the higher sodium, calcium and magnesium content of SAFA.

Place table 3 here

Of the modified composites the m-PP modified samples were least effected, possibly because not all the adsorption sites on the fly ash surfaces were occupied by the relatively widely spaced pendent anhydride groups of m-PP. Such patchy adsorption allowed the same AO-filler interactions to occur as with the unmodified composite. The other surface modifiers led to increased melt stability at 160 ºC. This was particularly true of γ-MPS/DCP and BMI/DCP modifications that led to greater than four-fold increases in OIT relative to the unfilled matrix. The C800/DCP modification led to near two-fold increases in OIT. Differences arising from the type of fly ash were small (and arguably within experimental error) in the modified composites. Considering the addition of DCP to the BMI, γ-MPS and C800 modification systems, it is surprising that any enhanced thermal stability occurred at all, as some chain scission and consumption of stabiliser would be expected as a result of the DCP reactions. Chain scission was probably manifested as an increase in VMFR (Figure 4). This effect was particularly obvious with the C800/DCP modifications. The increase in melt stability is therefore likely to be related to tethering of PP chains to the filler surface and blockage of stabiliser adsorption sites on the filler surface. In the case of m-PP, the mechanical

property data and fracture surface images suggest good interfacial adhesion[16]. However, this is achieved via a very different mechanism to that associated with free radical addition polymerisation of active double bonds of coupling agent molecules. In the latter systems the coupling density to the filler surface may be relatively high, whilst with m-PP the coupling density may be somewhat lower, though coupling is bolstered by transcrystallisation and chain entrapment.

Place Figure 4 here

The increased value of VMFR of the SAFA based C800/DCP and m-PP modified composites, relative to the equivalents based on UKFA supports the idea that interaction of these surface modifiers with SAFA resulted in a greater amount of ion extraction and hence loss of filler-matrix interaction. This effect is particularly significant with m-PP as reaction of both acid groups formed (as a result of ring opening of the pendent anhydride) could react with the same Ca^{2+} (and/or Mg^{2+} but to a lesser extent considering the ICP data (Table3)) ion and remove it from the fly ash surface. For steric reasons this effect with Ca^{2+} / Mg^{2+} may be less prevalent with C800. The γ-MPS / DCP modified composites follow the same trend but to a lesser extent than with C800 / DCP. This is due to the ability of the silane to interact with Si-OH as well as metal (M)-OH; a silicon atom cannot be removed in the same way as a metal ion. Therefore the silane is more likely to remain attached to the fly ash surface. This may explain why the VMFR for the γ-MPS modified composites is lower than that for the C800 modified composites; true coupling occurred to a greater extent in the former. The BMI / DCP modification was affected adversely by the low melt temperature of the UKFA based composite as the temperature was too low to melt the BMI. This resulted in limited coupling and a greater amount of DCP induced PP chain scission. The slightly higher melt temperature of the SA4 based composite (possibly also combined with the higher pH of SA4) led to proper melting and significantly greater coupling, which led to the lowest recorded VMFR value for an SA4 based composite. The tetra functionality of BMI to macro-radicals (resulting in branching and crosslinking) also offset the viscosity reduction effect associated with beta scission of the PP matrix.

OIT data for the TSE-IM produced samples are shown in Figure 5.

Place Figure 5 here

The vast difference in the OIT data for the BM-CM and TSE-IM processed unfilled matrix samples is a manifestation of the vastly longer residence time and air exposure associated with the Haake mixing process. The OIT for the TSE-IM processed unfilled matrix sample was about twenty times higher than that produced via the BM-CM route. Almost all the stabiliser systems in the PP appeared to have been consumed during Haake processing. The OITs of the TSE-IM processed composites however, were much reduced; to the extent that they are similar to those of the BM-CM processed equivalents. Whilst the reductions were worryingly large, the UKFA gave consistently higher OIT in the TSE-IM produced composites. The C800/DCP modification led to an approximate trebling of the OIT relative to the unmodified composites. This increase in melt stability occurred despite possible chain scission. These observations reinforce the argument in favour of the need to tether matrix chains to filler surfaces, whilst blocking stabiliser adsorption sites, if good melt stability is a design objective.

 The superiority of the UKFA in terms of melt stability again indicates that the presence of appreciable water / acid leachable transition element content in fly ash does not necessarily result in poor matrix stability in a composite. The poor melt stability of the unmodified composites was most likely due to mechano-oxidative degradation associated with the higher shear stresses experienced by the polymer in a filled melt combined with loss of stabiliser via adsorption on the fly ash surfaces. C800/DCP modification brought about improvements, but they were nowhere near sufficient to boost melt stability up to that of the unfilled matrix.

Thermal oxidative degradation in the solid state

The carbonyl regions of ATR-FTIR spectra obtained for the oven aged BM-CM processed unfilled PP matrix are shown in Figure 6.

Place Figure 6 here

Even after just 16 hours at 150 ºC the carbonyl band has grown significantly, indicating rapid oxidation. The oxidation of PP is often accompanied by development of a yellow / brown colouration. This was also observed in the case of the BM – CM processed composite samples. Induction times to the onset of carbonyl growth $(t_{C=O})_{onset}$ and the values of carbonyl index obtained after 2 and 8 hours $((CI)_{2h}$ and $(CI)_{8h}$, respectively are shown in Figure 7.

Place Figure7 here.

The $(t_{C=O})_{onset}$ data shows that the addition of SAFA did not prevent initiation of thermal oxidation of the matrix. However, all the surface modifiers, with the exception of m-PP, led to a significant retardation of initiation. With γ-MPS/DCP modification a five – fold increase in $(t_{C=O})_{onset}$ was observed. Once carbonyl growth was established only the γ - MPS/DCP led to a reduction in $(CI)_{8h}$, relative to the unfilled matrix. The other surface modifiers led to a significant increase in $(CI)_{8h}$. The unmodified composite also had slightly higher $(CI)_{8h}$ than the unfilled matrix, therefore indicating the SAFA had a mild pro-degradation effect once oxidation had been initiated.

Values of $(t_{C=O})_{onset}$, $(CI)_{2h}$ and $(CI)_{8h}$ for the UKFA based composites produced via the Haake-CM route are shown in Figure 7. Whilst unmodified UKFA appeared to promote a longer $(t_{C=O})_{onset}$ than the unfilled matrix, the $(CI)_{8h}$ value was slightly higher than that of the unmodified SAFA based composite. The retarded initiation of oxidation arising from addition of UKFA is also consistent with the OIT data. These observations may be related to differing interactions of the fly ash samples with the PP stabilisers. The UKFA based surface modified composites showed generally higher values of $(t_{C=O})_{onset}$, with the C800/DCP modification giving by far the best performance in this respect. However, once oxidation started, the extent of degradation of composites modified with γ -MPS/DCP, BMI/DCP and m-PP was somewhat higher relative to those based on SAFA. The latter observations were not captured in the $(CI)_{8h}$ data, but are evident towards the end of the 16 hour ageing period. In UKFA the C800/DCP modification offered the best enhancement of thermal oxidative stability.

The TSE-IM processed UKFA and SAFA based composites were also oven aged at 150 ºC and the oxidation was followed using the same ATR-FTIR method. Values of $(t_{C=O})_{onset}$ and $(CI)_{8h}$ are given in Table 4.

Place Table 4 here

The $(t_{C=O})_{onset}$ trends followed the OIT trends in Figure 3. The degradation of the unfilled matrix was not initiated during the 10 hour ageing period and the UKFA promoted greater retardation of initiation of oxidation than SAFA, whilst the C800/DCP modification led to slightly increased values of $(t_{C=O})_{onset}$. An explanation of these effects is given earlier, and is related to possible preferential adsorption of stabilisers on

SAFA, and the effect of C800 blocking of stabiliser adsorption sites. The latter together with tethering of PP chains to the fly ash surface, possibly led to the slightly increased $(t_{C=O})_{onset}$ values. SAFA also gives rise to a higher rate of oxidation, which after ca. 6 hours is overtaken by the C800/DCP modified SAFA based composite. After the 10 hour ageing period the latter composite has undergone the highest extent of oxidation by a large margin. In contrast, the C800/DCP modification of the UKFA based composites did not significantly affect the extent of oxidation. In the case of the SAFA based composites, once oxidation had been initiated, it is likely that the residual DCP contributed to the largest extent of the oxidation observed with the C800/DCP modified composite. The latter may have been exacerbated by desorption of the C800-PP adducts (together with sodium, calcium and magnesium ions) from the SAFA surface during the course of ageing. Any remaining stabiliser may have been adsorbed (and effectively removed) on the pristine surface exposed by such desorption. The SEM images of the fracture surfaces (Figure 8) and mechanical property data obtained for the equivalent UKFA based composites suggests stronger adhesion of the interfacial region to the filler surface. Therefore the effect of residual DCP may have been countered by a greater concentration of stabiliser being available.

Place Figure 8 here.

Photo oxidative degradation in the solid state

Values of CI_{200h} and CI_{800h} for the photo-oxidation of the BM – CM processed SAFA based composites are given in Table 5.

Place Table 5 here

There was no photo-oxidation induction time in all samples apart from that based on unmodified SAFA where a short induction time of about 55 hours was estimated. However, once degradation had commenced, the carbonyl index of the latter composite increased rapidly. Once 200 hours of exposure had elapsed, the photo-oxidation trend for the unmodified SAFA based composite overtook all the samples apart from the C800/DCP, BMI/DCP and m-PP modified composites. At 800 hours exposure, the following order of decreasing carbonyl index was found:

m-PP > unmodified SAFA > γ-MPS/DCP > C800/DCP ≈ unfilled PP >BMI/DCP

As with the thermal stabilisation data, this ranking indicates that tethering of PP chains to the filler surface using a reactive surface modifier system, together with blockage of stabiliser adsorption sites, favours improved UV stability.

Values of $(t_{C=O})_{onset}$ together with CI_{200} and CI_{800} values for the UKFA based composites are given in Table 6.

Place table 6 here

With these composites, greater inherent stability made it possible to resolve induction times for the onset of carbonyl growth. It is immediately evident that the extent of photo-oxidation was lower with the UKFA based composites than those based on SAFA. All the composites showed a lower extent of oxidation than the unfilled matrix. All the surface modifiers led to similar levels of reduced stability relative to the unmodified composite.

Values of $(t_{C=O})_{onset}$, CI_{200h} and CI_{500h} for the TSE-IM processed composites are given in Table 7.

Place Table 7 here

The pro-photodegradation effect of both fillers (as compared using $(t_{C=O})_{onset}$ values) is evident, though the UKFA was certainly not as bad as SAFA in this respect. At more extended exposure periods the UKFA based composites appeared more stable than the unfilled matrix. As previously discussed, this effect is most likely related to the different interactions of the fly ash samples with the polymer stabilsers (i.e. it is proposed that UKFA adsorbs less of the stabilisers than SAFA) and not related to the higher transition metal content of UKFA. If the latter impurities were extractable by the polymer melt, the UKFA may well have been the worse performer. C800/DCP modification of the SAFA based composite had no significant effect on the initiation of photo-oxidation. However, towards the end of the exposure period, the C800/DCP modification resulted in reduced stability. The latter modification slighty reduced the $(t_{C=O})_{onset}$ of the UKFA based composite, though the data soon merged with the respective unmodified composite. The photo-oxidation trends observed with the C800/DCP modified composites were largely consistent with the thermal oxidation and mechanical property trends. The C800/DCP modified interfacial region was more strongly bonded to the UKFA surface than the SAFA surface. This effect led to the observed trends via the speculated mechanism proposed earlier.

Conclusions

The following conclusions can be derived from this investigation:

1. Addition of unmodified SAFA was found to accelerate degradation of PP, whilst addition of UKFA led to a weak pro-degradation effect and in some cases showed some stabilisation activity. This is slightly unexpected taking into account the higher detectable transition metal content of UKFA. The higher sodium, calcium and magnesium content of SAFA, may be related to a greater tendency to adsorb the antioxidants relative to UKFA.

2. The addition of SAFA did not affect the initiation of thermal oxidation of the matrix. However, it had a mild pro-degradation effect once oxidation had been initiated. All the surface modifiers, with the exception of m-PP, led to a significant retardation of degradation initiation.

3. The UKFA retarded the initiation of degradation. However, once oxidation got underway, the extent of degradation of composites modified with γ-MPS/DCP, BMI/DCP and m-PP, was somewhat higher relative to those based on SAFA.

4. In UKFA the C800/DCP modification offered the best enhancement of thermal oxidative stability.

5. Although the SAFA unmodified composite was the only material which gave a short photo-oxidation induction time, once degradation had commenced the carbonyl index of the latter composite increased rapidly. The extent of photo-oxidation was lower with the UKFA based composites.

6. All the composites showed a lower extent of oxidation than the unfilled matrix.

7. The composites had similar levels of reduced stability relative to the unmodified composite.

8. In the case of TSE-IM produced samples, the pro-photodegradation effect of both fly ash types is evident, though the UKFA was certainly not as bad as SAFA in this respect.

9. At more extended exposure periods the UKFA based composites appeared more stable than the unfilled matrix.

10. Tethering of PP chains via a densely adsorbed carpet of coupling agent molecules favours increased thermal oxidative and photo oxidative stability, despite the fact that macro-radical grafting reactions to the coupling agents were peroxide initiated. The latter possibly led to varying levels of chain scission during melt blending. Dense adsorption of the coupling agent probably prevented loss of stabiliser from the formulation by adsorption on the fly ash.

11. Coupling of the matrix to the fly ash surfaces using maleic anhydride grafted PP led to similar levels of property improvements as obtained using the monomeric coupling agents. However, the extent of retardation of oxidation was nowhere near as significant. This was thought to be due to adsorption of stabilisers at areas of the fly ash particles which were not covered by the m-PP. The low grafting density of maleic anhydride will lead to compromised adsorption that will leave the majority of the fly ash surface in a pristine state.

References

1 Nielsen, L. E.; Landel, R. F. Mechanical properties of polymers and composites; 2ⁿᵈ Edition, CRC Press: Boca Raton, **1994**

2 Zuiderduin, W. C. J. ; Westzaan, C. ; Hhuetink J.; Gaymans, R. J. *Polymer* **2003**, *44 (1)*, 261-275

3 Morelli, C. L.; Pouzada, A. S.; Sousa, J. A. *J. Appl. Pol. Sci.* **2009**, *114 (6)*, 3592-3601

4 Tan S.; Tynçer, T. *J. Appl. Pol. Sci.* **2010**, *118 (5)*, 3034-3040

5 Rothon, R. N. Particulate-Filled Polymer Composites*;* 2ⁿᵈ Edition, Smithers RAPRA Technology: UK, **2003**

6 Xanthos, M. Functional Fillers for Plastics, Wiley-VCH: Weinheim, **2005**

7 Liauw, C. M.; Hurst, S. J.; Lees, G. C.; Rothon, R. N.; Dobson, D. C. *Plas. Rubb & Comp. Proc. & Appl.* **1995**, *24 (5)*, 249-260

8 Jiangqing, P.; Hongmei, X.; Juying, Q.*;* Jinfen C.; Zhenmin, M. *Pol. Degrad. & Stabil.*, **1991,** *33 (1)*, 67-75

9 Suradi, S.S.; Yunus, R.M.; Beg, M.D.H.; Rival M.; Yusof, Z.A.M. *J. Appl. Sci.* **2010,** *10 (24)*, 3271-3276

10 Chen, X.; Yu, J.; Guo, S. *J. Appl. Pol. Sci.* **2007,** *103 (3)*, 1978-1984

11 Chen, D.; Zhang, H.; Zheng, Q.; Liu, F.; Xu K.; Chen, M. *Pol. for Adv. Technol.* **2008,** *19 (9)*, 1353-1360

12 Seldén, R.; Nyström B.; Långström, R. *Pol. Comp.* **2004,** *25I (5)*, 543-553

13 Domininghaus, H. Plastics for Engineers: Materials, Properties, Applications, Hanser Publishers: Dusseldorf, **1988**

14 Tsuchiya, V.; Sumi, K. *J. Pol. Sci.* **1969**, *7 (7)*, 1599-1607

15 Carlsson, D. J.; Wiles, D. M. *J. Macromol. Sci. C: Pol. Rev.* **1976**, *14 (1)*, 65-106

16 Iraola-Arregui, I.; Liauw, C. M.; Potgieter, H. *Macromol. Mater. & Eng.* **2011**, *296 (9)*, 810-819

17 Svoboda, P.; Poongavalappil S.; Theravalappil, R.; Svobova, D.; Mokrejs, P.; Kolomaznik, K.; Ougizawa, T.; Inoue, T. *J. Appl. Pol. Sci.* **2011,** *121 (1)*, 521-530

18 Li, L.; de Jeu, W. H. *Macromol.* **2003**, *36 (13)*, 4862-4867

19 Singh, B.; Sharma, N. *Pol. Degrad & Stabil* **2008**, *93 (3)*, 561-584

20 Mourelatou, D. **2003**, Thesis, (PhD), Manchester Metropolitan University

21 Allen, N. S.; Hoang, E.; Liauw, C. M.; Edge, M. H.; Fontan, E. *Pol. Degrad. & Stabil.* **2001**, *72 (2)*, 367-376

22 Baumhardt-Neto, R.; De Paoli, L. *Pol. Degrad. & Stabil.* **1993,** *40 (1)*, 59-64

23 Rajakumar, K.; Sarasvathy, V.; Thamaraichelvan, A.; Chitra, R.; Vijayakumar, C.T. *J. Appl. Pol. Sci.* **2010,** *118 (5)*, 2601-2612

Figure Captions

Figure 1. ATR-FTIR spectra of thermo-oxidative degradation in which the peaks mentioned above have been indicated

Figure 2. Schematic plot showing the $(t_{C=O})_{onset}$ measurement calculation.

Figure 3. OIT values for the Haake-CM produced composites based on UKFA and SAFA

Figure 4. VMFR values for South African and Rocktron composites

Figure 5. OIT comparison of the oxidative stability of South African and Rocktron composites

Figure 6. ATR-FTIR spectra of the Haake –CM processed unfilled PP matrix showing the growth of the carbonyl IR absorption bands with increasing oven ageing time at 150º C.

Figure 7. Histogrammes comparing SAFA and UKFA produced via the Haake-CM route: (a) $(t_{C=O})_{onset}$, (b) $(CI)_{2h}$ and (c) $(CI)_{8h}$.

Figure 8. SEM micrographs of impact fractured surface of fly ash-PP composites

Table 1. Composite Formulations.

Composite	Fly ash (g)	PP (g)	Coupling agent (mmol)	DCP (g)
PP unfilled	-	54.1	-	-
PP/Unmodified FA*	38.3	38.3	-	-
PP/(C800/DCP - FA).	38.3	37.8	1.6	0.023
PP/(BMI/DCP – FA).	38.3	38.1	0.8	0.023
PP/(γ-MPS/DCP – FA)	38.3	37.9	1.6	0.023
PP/(m-PP – FA)	38.3	36.0	2.3 g	-

*FA – Fly ash, composites were prepared from SAFA and UKFA.

Table 2. IR regions to calculate the carbonyl index.

	Area in region	Baseline
Carbonyl peak $A_{C=O}$	1817.2-1562.6	1822.0-1566.5
Reference peak A_{C-H}	1494.6-1390.5	1494.6-1391.0

Table 3. ICP data obtained for UKFA and SAFA under different leaching conditions

Element	Element concentration (ppm)			
	Aqueous leaching ("surface" ions)		Nitric acid leaching (ions from interior of shell)	
	SAFA	UKFA	SAFA	UKFA
Ca	17.0	10.3	73.2	59.7
Mg	2.8	1.8	21.0	22.4
Na	4.5	5.3	18.2	23
S	28.5	10.4	32.8	14.3
Si	2.8	1.5	56.6	43.8

Table 4. Values of $(t_{C=O})_{onset}$ and $(CI)_{8h}$ for SAFA and UKFA based composites produced via the TSE-IM route

	$(t_{C=O})_{onset}$ (h)	$(CI)_{8h}$
Unfilled PP	>10	0.06
SAFA	2.9	6.25
UKFA	2.9	1.61
SAFA-C800/DCP	3.3	9.48
UKFA-C800/DCP	4.2	1.75

Table 5. Photo degradation CI_{200h} and CI_{800h} values for BM-CM processed SAFA based composites.

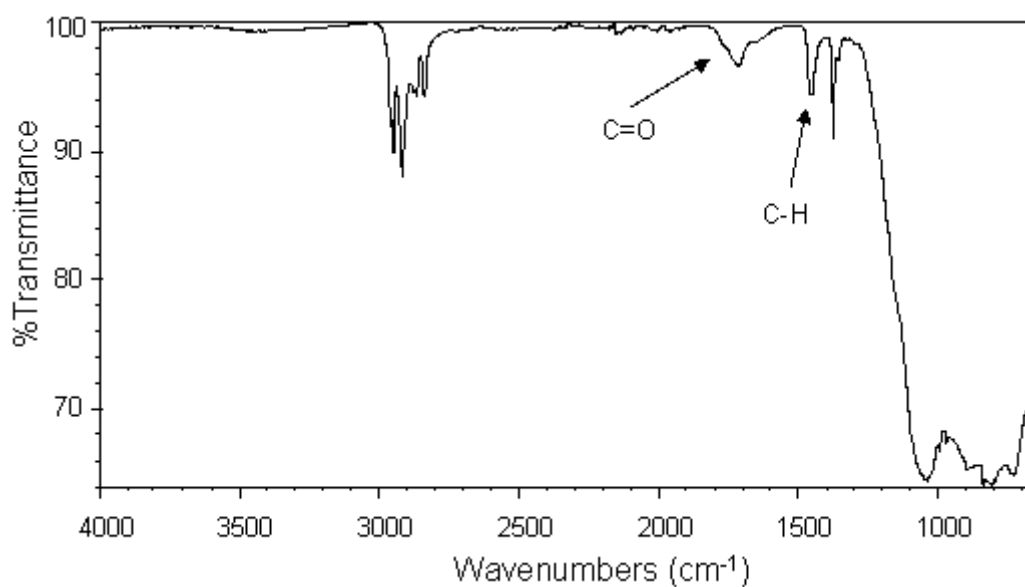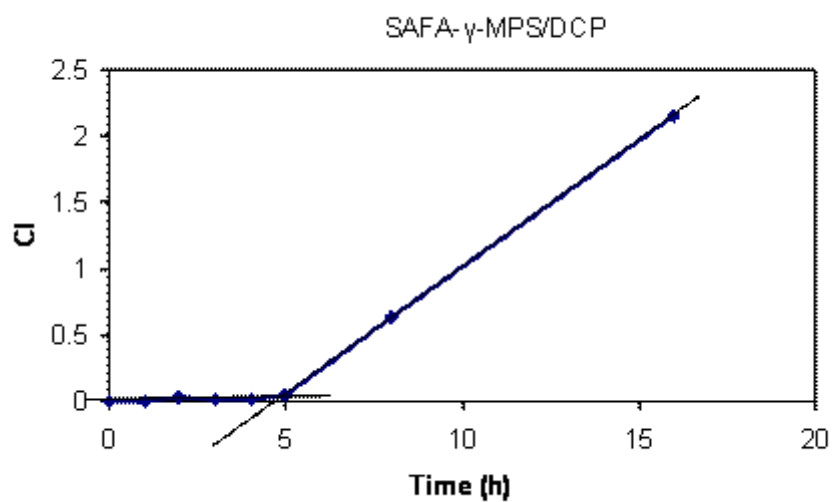|	CI_{200h}	CI_{800h}
Unfilled PP	0.45	1.46
SAFA	0.59	1.72
SAFA-C800/DCP	0.64	1.52
SAFA-BMI/DCP	0.56	1.41
SAFA-γ-MPS/DCP	0.48	1.57
SAFA-m-PP	0.67	1.86

Table 6. Photo degradation $(t_{C=O})_{onset}$, CI_{200h} and CI_{800h} values for BM-CM processed UKFA based composites.

	$(t_{C=O})_{onset}$ (h)	$(CI)_{200h}$	$(CI)_{800h}$
Unfilled PP	-	0.53	1.46
UKFA	130	0.35	1.22
UKFA-C800/DCP	135	0.26	1.26
UKFA-BMI/DCP	160	0.35	1.33
UKFA-γ-MPS/DCP	90	0.54	1.38
UKFA-m-PP	150	0.39	1.31

Table 7. Photo degradation $(t_{C=O})_{onset}$, CI_{200h} and CI_{800h} values for TSE-IM processed SAFA and UKFA based composites.

	$(t_{C=O})_{onset}$ (h)	$(CI)_{200h}$	$(CI)_{800h}$
Unfilled PP	280	0.03	2.09

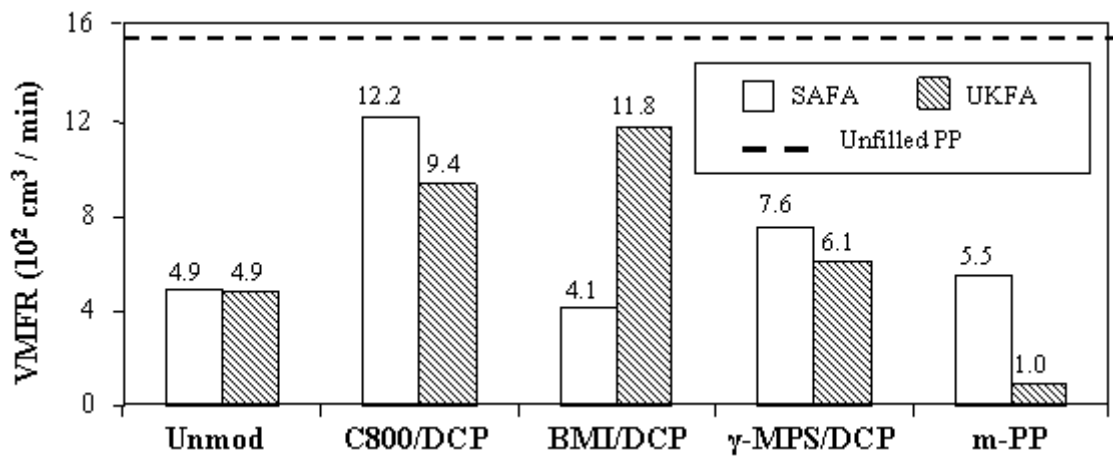|			
SAFA	100	0.70	2.46
UKFA	185	0.19	1.73
SAFA-C800/DCP	85	0.79	2.59
UKFA-C800/DCP	130	0.33	1.74

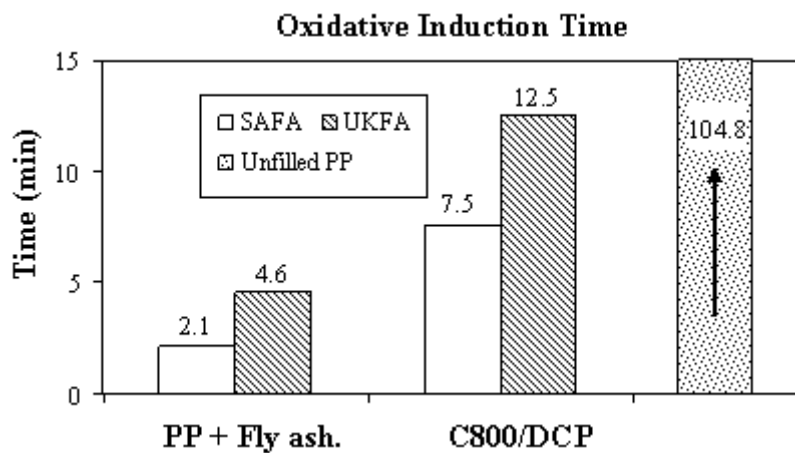**Figure 1.** ATR-FTIR spectra of thermo-oxidative degradation in which the peaks mentioned above have been indicated

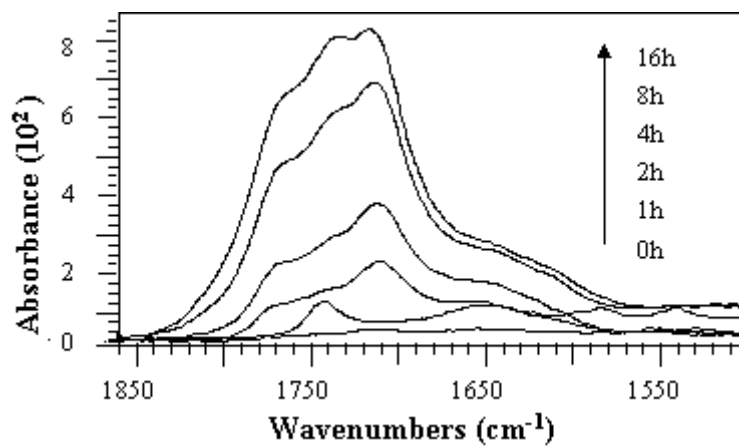**Figure 2.** Schematic plot showing the $(t_{C=O})_{onset}$ measurement calculation.

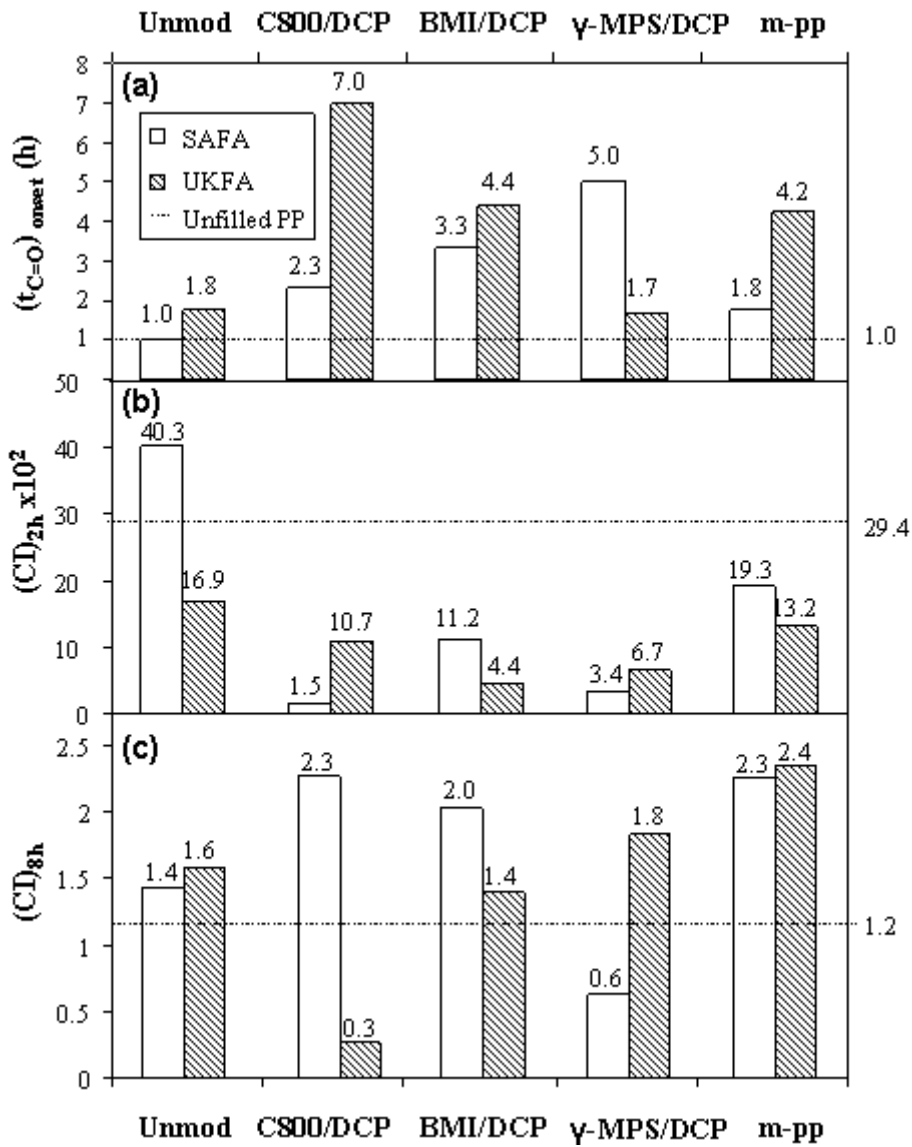**Figure 3.** OIT values for the Haake-CM produced composites based on UKFA and SAFA

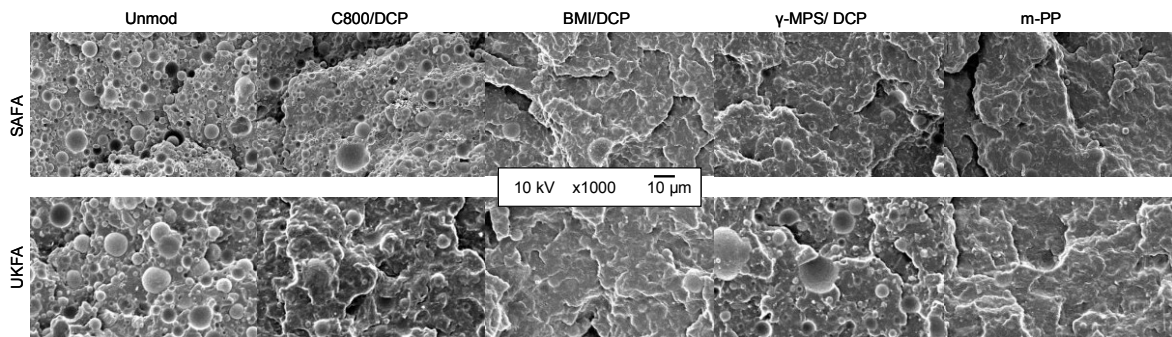**Figure 4.** VMFR values for South African and Rocktron composites.

Figure 6. ATR-FTIR spectra of the Haake –CM processed unfilled PP matrix showing the growth of the carbonyl IR absorption bands with increasing oven ageing time at 150º C.

Figure 7. Histogrammes comparing SAFA and UKFA produced via the Haake-CM route: (a) $(t_{C=O})_{onset}$, (b) $(CI)_{2h}$ and (c) $(CI)_{8h}$.

Figure 8. SEM micrographs of impact fractured surface of fly ash-PP composites